Journal of Materials Chemistry A

RSC Publishing

PAPER

View Article Online
View Journal | View Issue

Cite this: J. Mater. Chem. A, 2013, 1, 2211

Synthesis of aligned carbon nanotube composite fibers with high performances by electrochemical deposition†

Tao Chen, Zhenbo Cai, Longbin Qiu, Houpu Li, Jing Ren, Huijuan Lin, Zhibin Yang, Xuemei Sun and Huisheng Peng*

Received 9th November 2012
Accepted 6th December 2012

DOI: 10.1039/c2ta01039a

www.rsc.org/MaterialsA

To improve their practical applications, carbon nanotubes (CNTs) have recently been assembled into macroscopic fibers in which the CNTs are aligned to maintain their excellent properties. To further enhance the properties and expand the application of CNT fibers, it is critically important to introduce a second functional phase to produce high performance composite fibers. Herein, a general and efficient electrodeposition method has been developed to synthesize aligned CNT composite fibers into which a wide variety of components including metals and conductive polymers can be incorporated. The resulting composite fibers show remarkable mechanical and electrical properties, which enable promising applications in various fields. As a demonstration, CNT/silver composite fibers exhibit a high signal enhancement under weak laser irradiation when used as wire substrates for surface enhanced Raman scattering, and CNT/polyaniline composite fibers have been used to fabricate wire-shaped supercapacitors which achieve a specific capacitance of 2.26 mF cm^{-1}, at least two orders of magnitude greater than that of bare CNT fibers, and ten times that of other fiber materials, such as plastic wires coated with zinc oxide nanowires.

Introduction

Due to their unique structure and remarkable electrical, mechanical and thermal properties, carbon nanotubes (CNTs) have been widely explored for over two decades.[1–8] However, their practical use at the nanoscale remains challenging, considering that it is difficult to accurately control their structures and properties.[9] As a result, a lot of efforts have been devoted to assembling them into macroscopic architectures such as continuous fibers with diameters of micrometers and lengths of meters.[10–17] The CNTs are aligned to provide the fiber with a combined high electrical conductivity, mechanical strength, thermal stability and electrocatalytic activity. These fibers have been found to be promising for catalytic oxygen reduction reactions and wire-shaped photovoltaic devices.[18–20]

To further improve the properties and expand the application of CNT fibers, it is critically important to introduce a second functional phase to produce high performance composite fibers.[21–24] For instance, we have recently found that aligned CNT/poly(acrylic acid) composite fibers showed both higher tensile strength and electrical conductivity than bare CNT fibers,[25] while aligned CNT/polydiacetylene composite fibers showed an interesting electrochromatism which was not available to either CNT or polydiacetylene.[16] The above composite fibers have been typically synthesized by dipping bare CNT fibers into monomer or polymer solutions, followed by the evaporation of solvents. The second phases physically filled in the voids among the CNTs, and it was difficult for them to be uniformly dispersed in the composite fiber. In addition, a wide variety of functional components cannot be incorporated by this method. For instance, noble metal materials including silver (Ag) and gold (Au) nanoparticles have been widely investigated for surface enhanced Raman scattering and catalytic reactions, respectively,[26–28] and conductive polymers such as polyaniline (PANI) and polypyrrole (PPy) have been used extensively as electrode materials in lithium ion batteries and supercapacitors,[29–32] but it is difficult for either of them to be incorporated into CNT fibers by a solution coating process.

In this work, we have developed a general and efficient electrochemical method to synthesize aligned CNT composite fibers with excellent properties such as a combined high flexibility, tensile strength, electrical conductivity and electrocatalytic activity. The metal materials of Ag and Pt nanoaggregates and conductive polymers of PANI and PPy were mainly explored. As a demonstration of the application, CNT/Ag composite fibers were investigated as effective substrates for surface enhanced Raman scattering (SERS), while CNT/PANI composite fibers were used as electrodes to fabricate novel wire-shaped supercapacitors with high performance.

State Key Laboratory of Molecular Engineering of Polymers, Department of Macromolecular Science, Laboratory of Advanced Materials, Fudan University, Shanghai 200438, China. E-mail: penghs@fudan.edu.cn

† Electronic supplementary information (ESI) available: TEM image of CNTs, SEM images of CNT fibers, CNT/Ag and CNT/Pt composite fibers, and chemical structure of R6G. See DOI: 10.1039/c2ta01039a

Experimental section

Pyrrole was purified by vacuum distillation, and the other chemicals at analytical grade were used as received. Prior to electrochemical polymerization, a CNT fiber electrode for electrochemical deposition was typically fixed on glass with one end attached to a silver wire by silver paste to connect the external circuit. The electrochemical deposition was carried out in a three-electrode system (Fig. S1†), in which the CNT fiber, a platinum plate, and Ag/AgCl filled with a saturated KCl aqueous solution were used as the working, counter and reference electrodes, respectively.

CNT/Ag composite fibers were synthesized by a potentiostatic method at −0.4 V for different times ranging from 5 to 80 s. A 0.2 M KNO_3 aqueous solution containing 1 mM $AgNO_3$ was used as the electrolyte. Similarly, Ag nanoparticles could be also deposited onto the ITO conductive glass after it was cleaned with acetone and ethanol. CNT/Pt composite fibers were synthesized by a cyclic voltammetry (CV) method for different cycle numbers of 10–50 using a solution of 0.1 mM $H_2PtCl_6 \cdot H_2O$ in 0.1 M H_2SO_4 as the electrolyte. The potential was scanned from −1 to 0 V with a scan rate of 5 mV s^{-1}. The resulting CNT/Ag and CNT/Pt composite fibers were washed with de-ionized water, followed by drying in air.

CNT/PANI composite fibers were synthesized by a potentiostatic method using a CNT fiber as the working electrode at 0.75 V in an electrolyte solution (pH = 4.6) of 0.1 M aniline in 1 M H_2SO_4 for up to 1000 s. Similarly, CNT/PPy composite fibers were synthesized at 0.70 V in an electrolyte solution (pH = 3.5) of 0.1 M pyrrole in 0.1 M KNO_3 for up to 400 s. The resulting CNT/polymer composite fibers were also washed with de-ionized water, followed by drying in air.

A wire-shaped supercapacitor was fabricated by twisting together a CNT/PANI composite fiber coated with gel electrolyte and another CNT/PANI composite fiber. The gel electrolyte was composed of 10 g poly(vinyl alcohol) and 10 g phosphoric acid in 100 mL of water. During the fabrication, one end of the composite fiber coated with gel electrolyte was fixed on glass, and the second composite fiber was carefully twisted using tweezers. The wire-shaped supercapacitors based on bare CNT fibers were also fabricated by the same process.

The electrodeposition and electrochemical characterization were performed on a CHI 660d electrochemical workstation (Chenhua Instrument, China). The structures of the composite fibers were characterized by transmission electron microscopy (TEM, JEOL JEM-2100F operated at 200 kV) and scanning electron microscopy (SEM, Hitachi FE-SEM S-4800 operated at 1 kV). Mechanical tests were performed on a Shimadzu Table-Top Universal Testing Instrument, and the fiber used was mounted on a paper tab with a gauge length of 5 mm. Raman measurements were performed on a Renishaw inVia Reflex with an excitation wavelength of 514.5 nm and laser power of 20 mW. Electrical resistances were measured by a digital multimeter, and electrical conductivities were then calculated according to the equation $\sigma = RS/L$, where σ, R, S and L represent the electrical conductivity (S cm^{-1}), electrical resistance (Ω), cross-sectional area (cm^2) and length (cm), respectively.

Results and discussion

CNT fibers were prepared from spinnable CNT arrays by a dry spinning process.[13,16,17] The fiber diameter was controlled from several to tens of micrometers, and the length could reach hundreds of meters. In this work, multi-walled CNTs with diameter of ~8 nm were mainly studied (Fig. S2a†). The fiber was highly uniform in both structure and diameter (Fig. S2b and c†), and the CNTs were highly aligned with each other as expected. As a result, the fiber showed excellent electrical and mechanical properties, such as conductivities in the range of 10^2 to 10^3 S cm^{-1} and strengths of 10^2 to 10^3 MPa, and could be used as electrodes to deposit a second phase through an electrodeposition process.

Ag nanoparticles were electrodeposited onto the surface of the bare CNT fibers through a three-electrode system. Fig. 1 shows typical scanning electron microscopy (SEM) images of a CNT/Ag composite fiber after electrodeposition of 30 s. Ag nanoparticles with diameters of 30 to 60 nm were uniformly attached on the aligned CNTs (Fig. 1b and c). The content of the Ag nanoparticles was mainly controlled by varying the electrodeposition time (typically 5 to 80 s). Fig. S3† further shows SEM images of CNT/Ag composite fibers made with an increasing electrodeposition time of 0 to 80 s. The diameters of the Ag nanoparticles increased with the increasing time, possibly due to aggregation during the electrodeposition.

Pt nanosheets were produced on the surface of CNT fibers by a cyclic voltammetry method with different numbers of cycles (Fig. S4†). With the increase of the number of CV cycles from 10 to 30, the nanosheets further aggregated into larger flowers with sizes of 1 to 3 μm (Fig. S4e and f†). Interestingly, these flowers were typically oriented along the direction of the aligned CNTs (Fig. 2). With the further increase of the number of CV cycles to 50, the nanosheets aggregated into irregular morphologies, and the resulting fiber became non-uniform in diameter (Fig. S4g and h†).

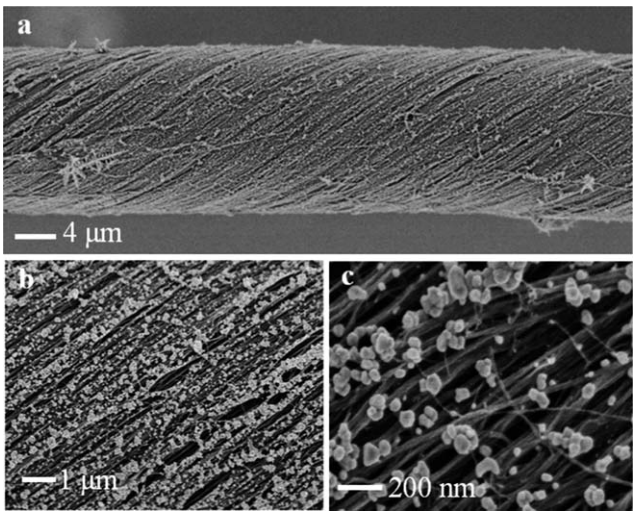

Fig. 1 Scanning electron microscopy (SEM) images of an aligned CNT/Ag composite fiber with an electrodeposition time of 30 s at (a) low and (b and c) high magnifications.

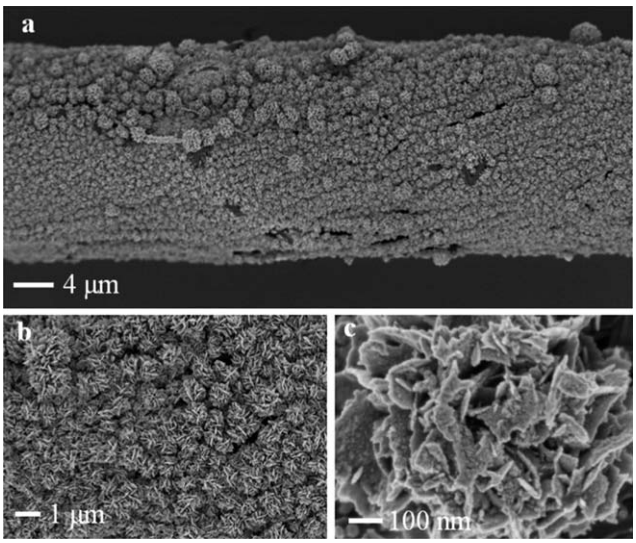

Fig. 2 SEM images of an aligned CNT/Pt composite fiber made with 40 CV cycles at (a) low and (b and c) high magnifications.

Fig. 3 shows SEM images of a CNT/PANI composite fiber synthesized by a potentiostatic method at 0.75 V for 1000 s. CNTs were uniformly coated with a layer of polymer, which could be clearly observed from the high magnification SEM images (Fig. 3b and c). Of course, the CNTs maintained their highly aligned structure after the incorporation of the polymer. PPy could also be uniformly deposited on the surfaces of CNTs in the fiber by the same process. Fig. 4 shows typical SEM images of the aligned CNT/PPy composite fibers with electrodeposition times of 80 and 160 s. With further increase of

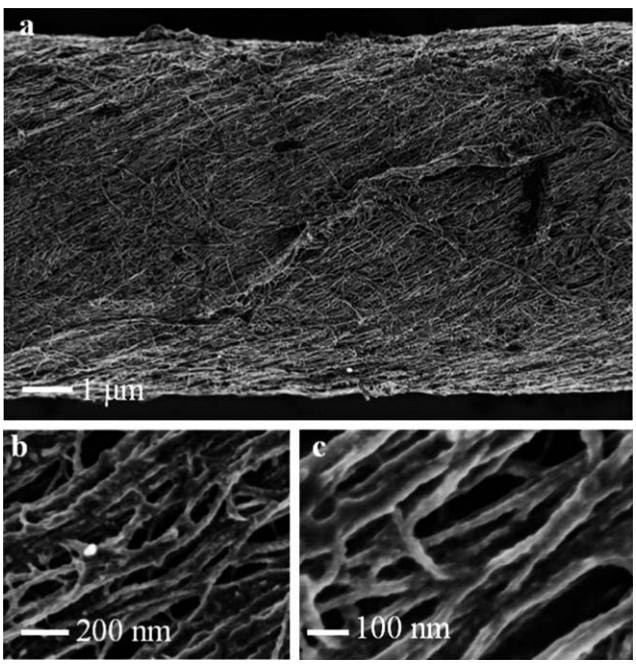

Fig. 3 SEM images of an aligned CNT/PANI composite fiber with an electrodeposition time of 1000 s at (a) low and (b and c) high magnifications.

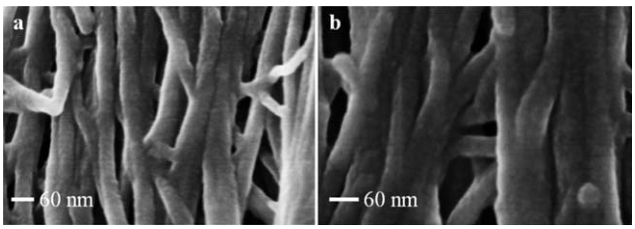

Fig. 4 SEM images of aligned CNT/PPy composite fibers with an electrodeposition time of (a) 80 s and (b) 160 s.

electrodeposition time, the additional conductive polymers were mainly coated as a thin layer on the outer surfaces of composite fibers, which largely decreased their electrical conductivities, which will be discussed later. Therefore, aligned CNT/polymer composite fibers with a uniform structure have mainly been studied if not specified.

The CNT composite fibers exhibited excellent mechanical and electrical properties (Fig. 5). For instance, compared with the bare CNT fiber, the strength was increased by over 30%, while the conductivity remained almost unchanged in the CNT/PPy composite fibers (Fig. 5a), and both strength and conductivity increased by as much as 70% and 30% for the CNT/PANI composite fibers, respectively (Fig. 5b). The strengths and conductivities of the different types of composite fibers are further compared in Table 1. The bare CNT fiber used in this work had a strength of 400 MPa. The strengths were slightly increased to 480 MPa (by 20%) and 410 MPa (by 2.5%) for the CNT/Ag and CNT/Pt composite fibers, respectively. As a strong contrast, the strength was greatly enhanced to 680 (by 70%) and 580 MPa (by 32%) in the CNT/PANI and CNT/PPy composite fibers, respectively. The different degrees of improvement may be attributed to the different structures. In the case of the metal materials, Ag nanoparticles or Pt aggregates were dispersed on the CNTs (Fig. 1 and 2), and the increase in strength was in fact mainly derived from the shrinkage of the CNT fibers in the

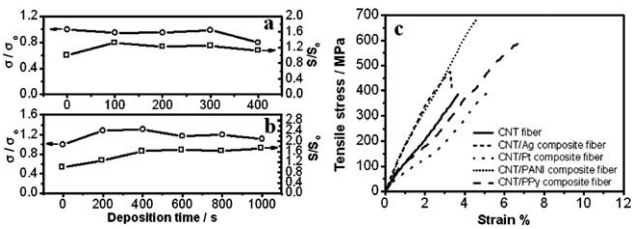

Fig. 5 Electrical and mechanical properties of different composite fibers. (a) Normalized electrical conductivity and tensile strength of CNT/PPy composite fibers with increasing electrodeposition time from 0 to 400 s. (b) Normalized electrical conductivity and tensile strength of CNT/PANI composite fibers with increasing electrodeposition times from 0 to 1000 s. Here, σ_0 and σ correspond to the conductivities before and after the electrodeposition of polymers, respectively. S_0 and S correspond to the strengths before and after the electrodeposition of polymers, respectively. Both conductivity and strength were calculated as average values from at least five samples. (c) Typical stress–strain curves of bare CNT and composite fibers. CNT/Ag, CNT/PANI and CNT/PPy composite fibers were synthesized by electrodeposition for 30, 1000 and 400 s, respectively. The CNT/Pt composite fiber was synthesized by electrodeposition for 40 CV cycles.

Table 1 Strengths and conductivities of bare CNT and composite fibers

Sample	Strength (MPa)	Conductivity (S cm^{-1})
CNT fiber	400 ± 20	215 ± 10
CNT/Ag fiber[a]	480 ± 15	220 ± 10
CNT/Pt fiber[b]	410 ± 15	240 ± 10
CNT/PANI fiber[c]	680 ± 20	230 ± 10
CNT/PPy fiber[d]	580 ± 20	170 ± 15

[a] Electrodeposition for 30 s. [b] Electrodeposition for 40 CV cycles. [c] Electrodeposition for 1000 s. [d] Electrodeposition for 400 s.

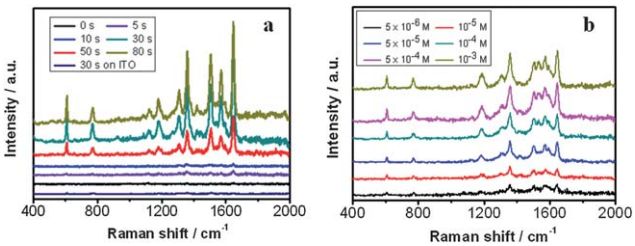

Fig. 6 (a) Raman spectra of 10^{-6} M R6G on the CNT/Ag composite fibers with electrodeposition times of 0 to 80 s, and the ITO substrate with 30 s electrodeposition. The laser power intensity and exposing time were 10 μW and 10 s, respectively. (b) Raman spectra of R6G with increasing concentrations of 5×10^{-5} to 1×10^{-3} M on a CNT/Ag composite fiber with an electrodeposition time of 30 s. The laser power intensity and exposing time were 200 μW and 10 s, respectively.

electrolyte solutions.[25] For PANI and PPy, polymer chains attached on CNTs were entangled to bundle neighboring CNTs more tightly (Fig. 3 and 4), which effectively prevented sliding between neighboring CNTs. As has been widely explored, CNT fibers are broken due to the sliding of CNTs, not the breaking of individual CNTs. Therefore, the aligned CNT/polymer composite fibers showed much increased strength.

As expected, conductivities were improved after incorporation of the metal materials Ag nanoparticles and Pt aggregates (Table 1). Interestingly, the CNT/Pt composite fibers exhibited higher conductivities than CNT/Ag, even though Ag has better conductivity than Pt. This phenomenon may be explained by the fact that isolated Ag nanoparticles were produced, but continuous Pt aggregates were formed on the surface of composite fibers (Fig. 1 and 2). In the case of conductive polymers, the conductivities of the composite fibers varied slightly compared with the bare CNT fibers.

Noble metals such as Ag have been widely investigated for SERS, and they typically appear in a planar format.[26–28] Due to their remarkable electrical and optical properties, CNTs have also been used to form composite materials with metals to prepare SERS substrates, with the aim of achieving higher efficiencies.[33,34] Herein, aligned CNT/Ag composite fibers were fabricated by an easy and low-cost electrochemical method, compared with the conventional lithography-based techniques and physical deposition, which may require complex process and high vacuum. In addition, the obtained CNT/Ag composite fiber had a larger surface area to adsorb more molecules with enhanced Raman signals. Here the sufficient "hot" sites of the metal nanoparticles also efficiently enhanced the Raman signal.[26–28] Rhodamine 6G (R6G), a well-studied probe molecule, was used to evaluate the effect of the SERS substrate in this work.[34] The as-prepared composite fiber was immersed into R6G solutions in ethanol with different concentrations. Fig. 6 shows the typical Raman spectra of R6G obtained with a concentration of 10^{-6} M under extremely weak laser irradiation of 10 μW. The peak at 1180 cm^{-1} was associated with a C–C stretching vibration, while the other peaks at 1310, 1362, 1506, 1572, and 1647 cm^{-1} were attributed to the C–C stretching vibrations of the aromatic unit.[35] The significant Raman enhancements are ascribed to the surface resonance Raman scattering derived from the interaction between the excitation wavelength and the excited electronic state of the R6G molecules.[35] The SERS signal intensity first increased with increasing electrodeposition time from 5 to 30 s, and then slightly decreased with the further increase of electrodeposition time to 50 s (Fig. 6a). This phenomenon is closely related to the different structures of the Ag nanoparticles in the composite fibers. They were uniformly dispersed for electrodeposition times less than 30 s, and then fused into larger and more irregular aggregates beyond this point (Fig. S3†). Therefore, the effective surface areas firstly increased and then slightly decreased, so the optimal electrodeposition time was 30 s.

Generally, the CNT fibers also showed characteristic Raman peaks at 1584 cm^{-1} for the G-band and 1350 cm^{-1} for the D-band (Fig. S5†). However, the Raman peaks of bare CNT fibers were very weak at the investigated low laser intensity (10 μW), and they could not be as clearly observed as those for the R6G-adsorbed CNT composite fibers, which were much stronger under the same conditions (Fig. 6a). In another control experiment, a piece of ITO conductive glass was electrodeposited with Ag nanoparticles under the same conditions and used as the SERS substrate. The control sample exhibited a much lower SERS effect than the CNT/Ag composite fibers. In addition, compared with the conventional planar SERS substrate, these wire-shaped substrates represent a novel format with unique advantages, such as being light-weight, weaveable and available for integration into complex structures.[20]

Electrochemical supercapacitors are also generally fabricated with a planar format, and cannot meet applications in a wide variety of fields which require them to be weaveable, *e.g.*, electronic textiles. Recently, some attempts had been made to prepare wire-shaped supercapacitors as a good solution to this problem.[36,37] Metal wires or plastic wires coated with a conducting layer (*e.g.*, indium tin oxide) were used as electrodes. However, the metal wires exhibited low flexibility and were easily corrupted by the electrolyte, while the conducting layer easily cracked and broke off the plastic wire. CNT fibers show high strengths and conductivities, and have been proved as effective electrodes for dye-sensitized solar cells.[18–20] Therefore, they may also be promising as electrodes for wire-shaped supercapacitors.

Here a wire-shaped supercapacitor was fabricated by twisting two bare CNT fibers or two composite fibers, followed by the

incorporation of a gel electrolyte (Fig. S6†). The electrochemical properties of the resulting supercapacitors were measured using a potentiostat/galvanostat. The supercapacitors based on both bare CNT and composite fibers were investigated carefully. Obviously, the CV curves (Fig. 7a) maintained their shape well with the increasing scan rate from 10 to 100 mV s^{-1}, which indicates good electrochemical stability. Fig. 7b shows a typical galvanostatic charge–discharge curve of a wire-shaped supercapacitor based on two CNT/PANI composite fibers with a charge–discharge current of 10 μA. For the wire-shaped supercapacitor, capacitance per unit length was used to characterize the device. The specific capacitance (C_L) was calculated by the equation $C_L = I\Delta t/L\Delta V$, where I, Δt, L and ΔV correspond to the current loaded (A), discharge time (s), length (cm) and potential window (V). The supercapacitor wire based on the CNT/PANI composite fiber achieved a capacitance of 2.26 mF cm^{-1}, at least two orders of magnitude greater than that of the bare CNT fibers (0.005–0.02 mF cm^{-1}, obtained from Fig. S7†), and ten times that of other fiber materials, such as plastic wires coated with zinc oxide nanowires (0.2 mF cm^{-1}).[36]

Conclusions

In summary, we have shown a concise synthesis of aligned CNT composite fibers incorporated with metal nanomaterials and conductive polymers by an electrochemical deposition method. The composite fibers were mechanically strong and electrically conductive, and could be widely used as a new family of substrates. As a demonstration, the CNT/Ag composite fiber was used as an effective SERS substrate and exhibited a high sensitivity and reproducibility in the detection of the R6G molecule at very weak laser irradiation, and CNT/PANI composite fibers were twisted into flexible and weaveable supercapacitors in a wire format with a high specific capacitance of 2.26 mF cm^{-1}. Compared with the widely explored planar counterparts, the wire-shaped SERS substrate and supercapacitor have been found to show some unique advantages, *e.g.*, they could be easily integrated into various portable devices and equipment by a conventional textile technique. More efforts are underway in this direction. Our work also provides an easy and low-cost approach to prepare high-performance CNT composite materials for use in novel devices.

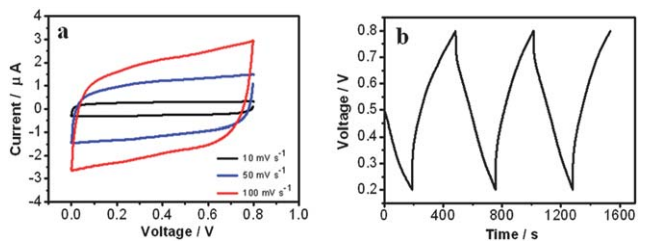

Fig. 7 (a) Cyclic voltammograms of a wire-shaped supercapacitor based on the CNT/PANI composite fiber with an electrodeposition time of 1000 s. (b) Galvanostatic charge–discharge curve measured at a current of 10 μA.

Acknowledgements

This work was supported by NSFC (91027025, 21225417), MOST (2011CB932503, 2011DFA51330), STCSM (11520701400, 12nm0503200) and The Program for Professor of Special Appointment (Eastern Scholar) at Shanghai Institutions of Higher Learning.

References

1 S. Iijima, *Nature*, 1991, **354**, 56–58.
2 T. W. Ebbesen, H. J. Lezec, H. Hiura, J. W. Bennett, H. F. Ghaemi and T. Thio, *Nature*, 1996, **382**, 54–56.
3 M.-F. Yu, O. Lourie, M. J. Dyer, K. Moloni, T. F. Kelly and R. S. Ruoff, *Science*, 2000, **287**, 637–640.
4 R. Martel, T. Schmidt, H. R. Shea, T. Hertel and P. Avouris, *Appl. Phys. Lett.*, 1998, **73**, 2447–2449.
5 V. Derycke, R. Martel, J. Appenzeller and P. Avouris, *Nano Lett.*, 2001, **1**, 453–456.
6 A. Bachtold, P. Hadley, T. Nakanishi and C. Dekker, *Science*, 2001, **294**, 1317–1320.
7 Y. Li, X. J. Huang, S. H. Heo, C. C. Li, Y. K. Choi, W. P. Cai and S. O. Cho, *Langmuir*, 2007, **23**, 2169–2174.
8 Y. Li, N. Koshizaki, H. Wang and Y. Shimizu, *ACS Nano*, 2011, **5**, 9403–9412.
9 R. Van Noorden, *Nature*, 2011, **469**, 14–16.
10 L. Liu, W. Ma and Z. Zhang, *Small*, 2011, **7**, 1504–1520.
11 K. Jiang, J. Wang, Q. Li, L. Liu, C. Liu and S. Fan, *Adv. Mater.*, 2011, **23**, 1154–1161.
12 K. Koziol, J. Vilatela, A. Moisala, M. Motta, P. Cunniff, M. Sennett and A. Windle, *Science*, 2007, **318**, 1892–1895.
13 Y.-L. Li, I. A. Kinloch and A. H. Windle, *Science*, 2004, **304**, 276–278.
14 M. Zhang, K. R. Atkinson and R. H. Baughman, *Science*, 2004, **306**, 1358–1361.
15 B. Vigolo, A. Pénicaud, C. Coulon, C. Sauder, R. Pailler, C. Journet, P. Bernier and P. Poulin, *Science*, 2000, **290**, 1331–1334.
16 H. Peng, X. Sun, F. Cai, X. Chen, Y. Zhu, G. Liao, D. Chen, Q. Li, Y. Lu, Y. Zhu and Q. Jia, *Nat. Nanotechnol.*, 2009, **4**, 738–741.
17 H. Peng, M. Jain, Q. Li, D. E. Peterson, Y. Zhu and Q. Jia, *J. Am. Chem. Soc.*, 2008, **130**, 1130–1131.
18 T. Chen, Z. Cai, Z. Yang, L. Li, X. Sun, T. Huang, A. Yu, H. G. Kia and H. Peng, *Adv. Mater.*, 2011, **23**, 4620–4625.
19 T. Chen, S. Wang, Z. Yang, Q. Feng, X. Sun, L. Li, Z. Wang and H. Peng, *Angew. Chem., Int. Ed.*, 2011, **50**, 1815–1819.
20 T. Chen, L. Qiu, Z. Yang, Z. Wang and H. Peng, *Nano Lett.*, 2012, **12**, 2568–2572.
21 H. G. Chae, M. L. Minus, A. Rasheed and S. Kumar, *Polymer*, 2007, **48**, 3781–3789.
22 A. Cayla, C. Campagne, M. Rochery and E. Devaux, *Synth. Met.*, 2012, **162**, 759–767.
23 J. Foroughi, G. M. Spinks, S. R. Ghorbani, M. E. Kozlov, F. Safaei, G. Peleckis, G. G. Wallace and R. H. Baughman, *Nanoscale*, 2012, **4**, 940–945.

24 L. K. Randeniya, A. Bendavid, P. J. Martin and C.-D. Tran, *Small*, 2010, **6**, 1806–1811.
25 W. Guo, C. Liu, X. Sun, Z. Yang, H. G. Kia and H. Peng, *J. Mater. Chem.*, 2012, **22**, 903–908.
26 C. Zhu, G. Meng, Q. Huang, Z. Zhang, Q. Xu, G. Liu, Z. Huang and Z. Chu, *Chem. Commun.*, 2011, **47**, 2709–2711.
27 L. Lu, G. Sun, H. Zhang, H. Wang, S. Xi, J. Hu, Z. Tian and R. Chen, *J. Mater. Chem.*, 2004, **14**, 1005–1009.
28 X. Xia, J. Zeng, B. McDearmon, Y. Zheng, Q. Li and Y. Xia, *Angew. Chem., Int. Ed.*, 2011, **50**, 12542–12546.
29 J. Zhang, L.-B. Kong, B. Wang, Y.-C. Luo and L. Kang, *Synth. Met.*, 2009, **159**, 260–266.
30 G. K. Ramesha, A. V. Kumara and S. Sampath, *J. Phys. Chem. C*, 2012, **116**, 13997–14004.
31 G. Lu, C. Li and G. Shi, *Polymer*, 2006, **47**, 1778–1784.
32 J. Wang, Y. Xu, J. Zhu and P. Ren, *J. Power Sources*, 2012, **208**, 138–143.
33 H. Zhao, H. Fu, C. Tian, Z. Ren and G. Tian, *J. Colloid Interface Sci.*, 2010, **351**, 343–347.
34 Y. Sun, K. Liu, J. Miao, Z. Wang, B. Tian, L. Zhang, Q. Li, S. Fan and K. Jiang, *Nano Lett.*, 2010, **10**, 1747–1753.
35 L.-B. Luo, L.-M. Chen, M.-L. Zhang, Z.-B. He, W.-F. Zhang, G.-D. Yuan, W.-J. Zhang and S.-T. Lee, *J. Phys. Chem. C*, 2009, **113**, 9191–9196.
36 J. Bae, M. K. Song, Y. J. Park, J. M. Kim, M. Liu and Z. L. Wang, *Angew. Chem., Int. Ed.*, 2011, **50**, 1683–1687.
37 J. A. Lee, M. K. Shin, S. H. Kim, S. J. Kim, G. M. Spinks, G. G. Wallace, R. Ovalle-Robles, M. D. Lima, M. E. Kozlov and R. H. Baughman, *ACS Nano*, 2012, **6**, 327–334.

